Chemistry & Biology, Volume *19*

Supplemental Information

Fluorescent Saxitoxins for Live Cell Imaging of Single Voltage-Gated Sodium Ion Channels beyond the Optical Diffraction Limit

Alison E. Ondrus, Hsiao-lu D. Lee, Shigeki Iwanaga, William H. Parsons, Brian M. Andresen, W.E. Moerner, and J. Du Bois

Inventory of Supplemental Information

Supplemental Data

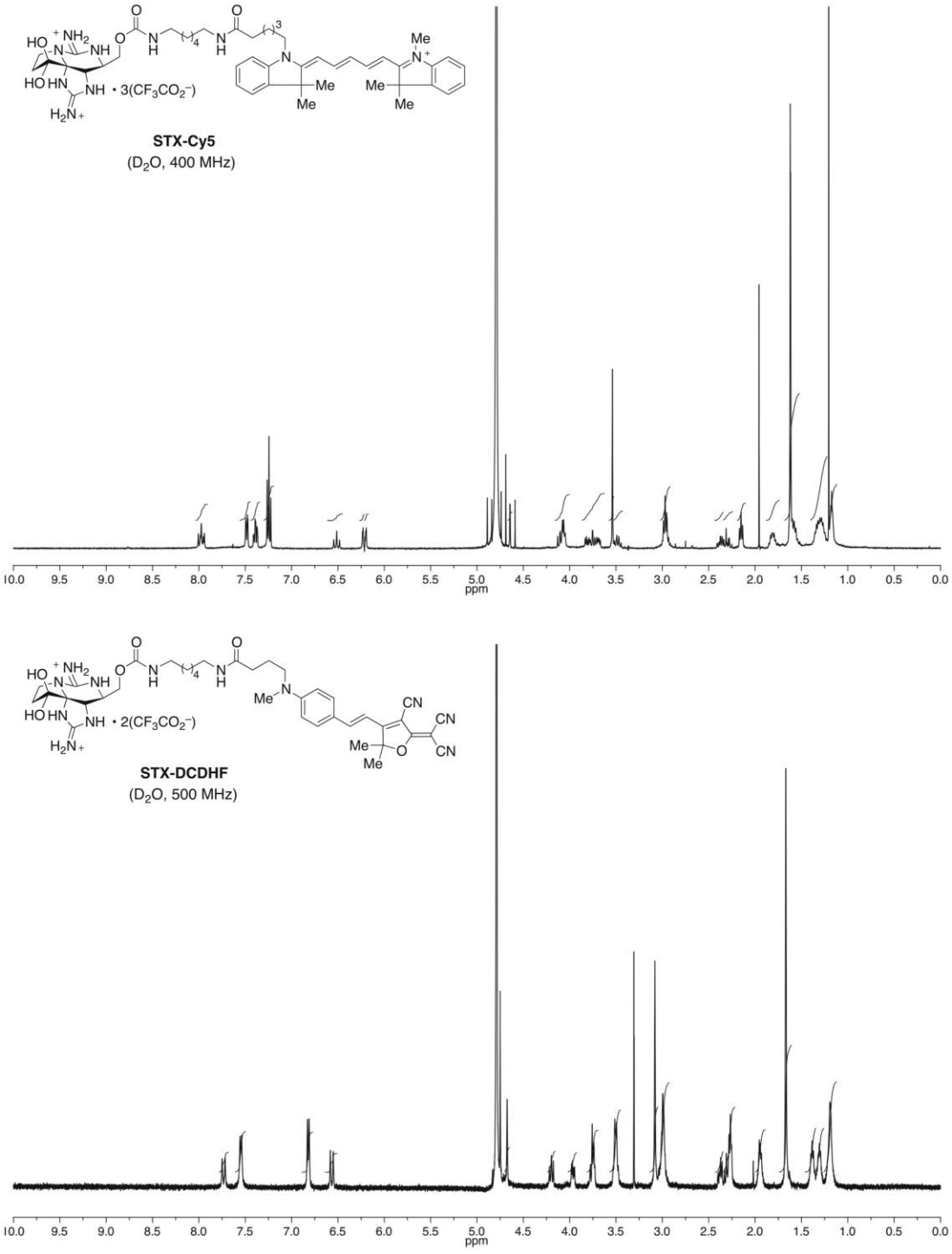

Figure S1, related to Figure 1. ^{1}H NMR spectra of STX-Cy5 and STX-DCDHF

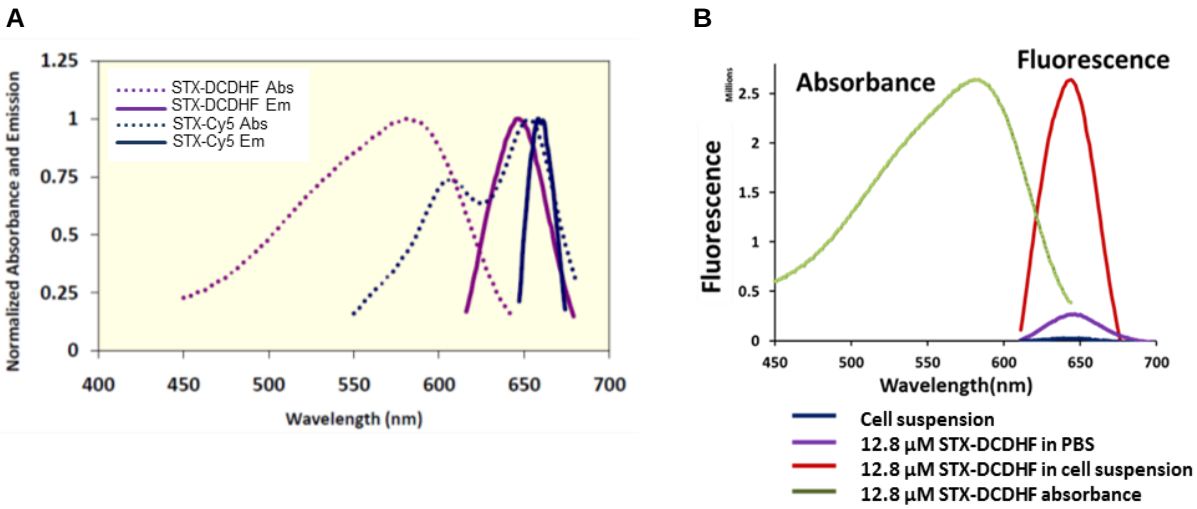

Figure S2, related to Figure 1. Fluorescence Properties of STX-Cy5 and STX-DCDHF

(**A**) Absorbance/emission spectra of **STX-Cy5** and **STX-DCDHF**. Absorbance (Abs, dotted lines) and emission (Em, solid lines) of **STX-Cy5** (blue) and **STX-DCDHF** (violet) in PBS solution at pH 7.4. **STX-Cy5**, $\lambda_{abs/em}$ = 655/665 nm; **STX-DCDHF**, $\lambda_{abs/em}$ = 580/640 nm. (**B**) Fluorescence enhancement of **STX-DCDHF** in cell suspension. 12.8 µM **STX-DCDHF** was used. The figure shows the relative fluorescence enhancement (~10×) in cell suspension (red line) compared to PBS (violet line) as a result of the viscosity/polarity sensitivity of the DCDHF chromophore. PBS = phosphate buffered saline.

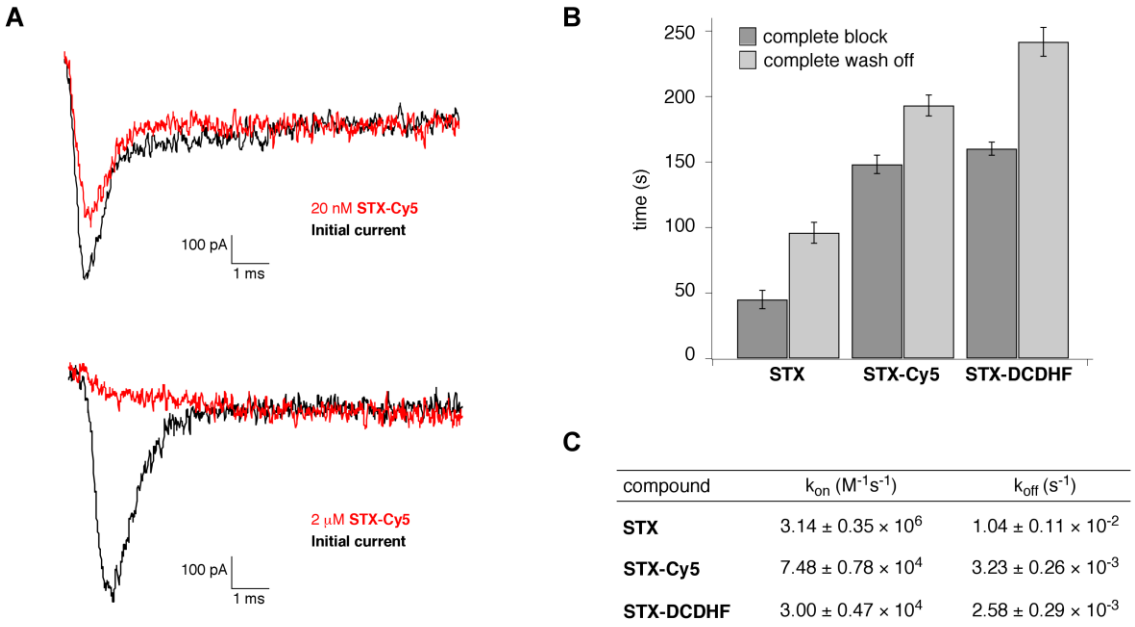

compound	k_{on} ($M^{-1}s^{-1}$)	k_{off} (s^{-1})
STX	$3.14 \pm 0.35 \times 10^{6}$	$1.04 \pm 0.11 \times 10^{-2}$
STX-Cy5	$7.48 \pm 0.78 \times 10^{4}$	$3.23 \pm 0.26 \times 10^{-3}$
STX-DCDHF	$3.00 \pm 0.47 \times 10^{4}$	$2.58 \pm 0.29 \times 10^{-3}$

Figure S3, related to Figure 1. Sample Electrophysiology Traces, On/Off Times, and Rate Constants for Na^+ Current Block by STX Toxins

(**A**) Sample electrophysiology traces acquired from whole-cell recordings on NGF-treated PC12 cells showing current block by **STX-Cy5**. (**B**) Measured τ_{on} and τ_{off} values for Na^+ current block on application of 2.0 μM toxin solutions. (**C**) Tabulated k_{on} and k_{off} values (equations from Hahn and Strichartz, 1981).

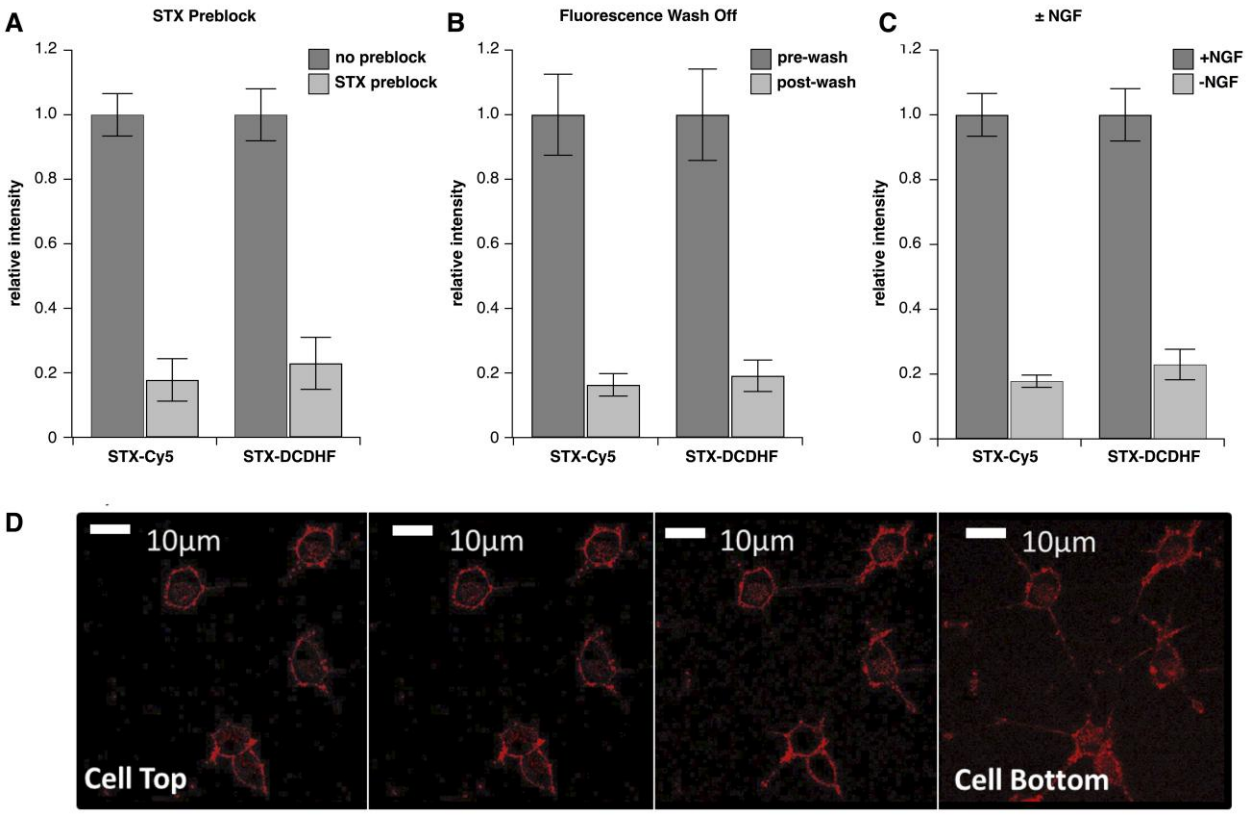

Figure S4, related to Figure 2. STX Pre-block, Probe Wash Off, and PC12 ± NGF Fluorescence, and Extracellular Labeling using STX-Cy5 and STX-DCDHF

(**A**)–(**C**) Quantification of STX pre-block, probe wash off, and PC12 ± NGF fluorescence. Media contained 10 nM **STX-Cy5** or 15 nM **STX-DCDHF**; in addition, media for pre-block and probe wash off contained 100 ng/mL NGF, and media for pre-block contained 10 µM STX. (**A**) Relative fluorescence of NGF differentiated cells before and after 3× media replacement. (**B**) Relative fluorescence of undifferentiated and NGF differentiated PC12 cells. (**C**) Relative fluorescence of samples of cells in media containing **STX-Cy5** and **STX-DCDHF** with and without blocking STX. (**D**) Confocal microscopy images. Extracellular labeling of NGF differentiated PC12 cells by **STX-DCDHF** after 3 h incubation. Media contained 15 nM **STX-DCDHF**. Representative z-stack images from near the top to the bottom of the cells acquired after 3 h incubation at 37 °C show that labeling is restricted to the outer membrane.

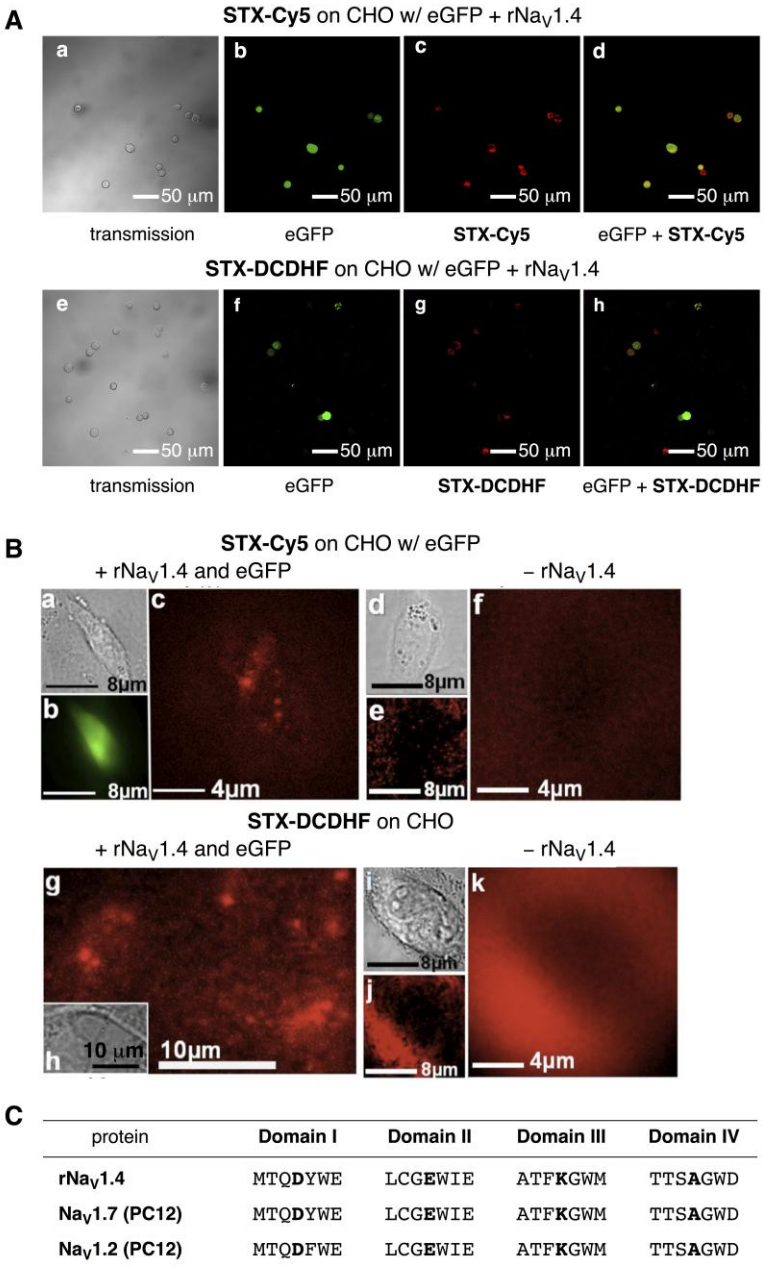

protein	Domain I	Domain II	Domain III	Domain IV
rNaV1.4	MTQ**D**YWE	LCG**E**WIE	ATF**K**GWM	TTS**A**GWD
NaV1.7 (PC12)	MTQ**D**YWE	LCG**E**WIE	ATF**K**GWM	TTS**A**GWD
NaV1.2 (PC12)	MTQ**D**FWE	LCG**E**WIE	ATF**K**GWM	TTS**A**GWD

Figure S5, related to Figure 2. Evaluation of Selective rNa$_V$1.4 Labeling by STX-Cy5 and STX-DCDHF in CHO Cells

(**A**) Confocal images of selective rNa$_V$1.4 labeling by STX-fluorophores in CHO cells. Cells were transfected with rNa$_V$1.4 and eGFP. Media for CHO cells contained 40 nM **STX-Cy5** or 60 nM **STX-DCDHF**. (a) Transmission image of CHO cells transfected with eGFP and rNa$_V$1.4. (b) eGFP fluorescence image of (a). (c) **STX-Cy5** fluorescence image of (a). (d) Merge of (b) and (c). (e–h) Corresponding images of cells treated with **STX-DCDHF**. (**B**)

Wide-field epifluorescence single-molecule images of selective rNa$_V$1.4 labeling by STX-fluorophores in CHO cells. Media contained 15 nM **STX-Cy5** or 100 nM **STX-DCDHF**. (a) Transmission image of a representative CHO transfected with both eGFP and rNa$_V$1.4. (b) eGFP fluorescence image of (a). (c) **STX-Cy5** fluorescence image of (a). (d) transmission image of a wild-type CHO cell. (e) **STX-Cy5** fluorescence image at the coverglass supporting the cell in (d). (f) **STX-Cy5** fluorescence of the cell in (d) showing no labeling at the apical membrane. (g)–(k) Corresponding images of cells treated with **STX-DCDHF**. For (f) and (k), diffuse fluorescence arises from **STX-DCDHF** in solution and adhered to the fibronectin-coated coverglass. (**C**) Sequence comparison of the pore region in rNa$_V$1.4, Na$_V$1.7 (PC12), and Na$_V$1.2 (PC12). Amino acid sequences in the STX binding site are identical.

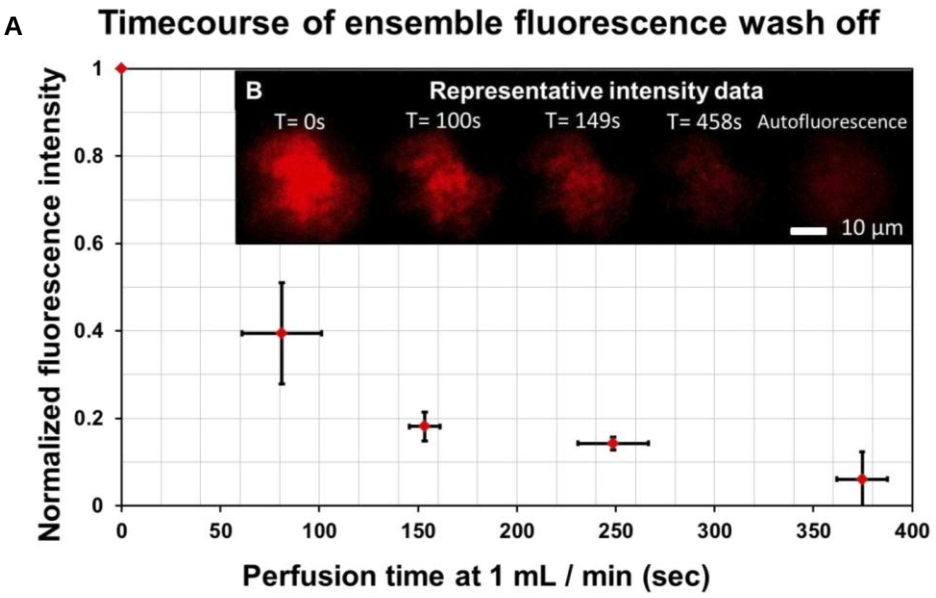

Figure S6, related to Figure 2. Average Time-Course of Ensemble Fluorescence Wash Off of STX-Cy5

(**A**) Each time-course is composed of a series of (time, normalized intensity) coordinates. The averaged time-course is a series of (averaged time point, averaged normalized intensity). The figure presented here represents data from three independent trials conducted with separate samples. Horizontal error bars represent the standard deviation of the averaged time points; vertical error bars represent the standard deviation of the averaged normalized intensities. (**B**) Representative intensity data taken over a single PC12 cell surface using wide-field epifluorescence microscopy.

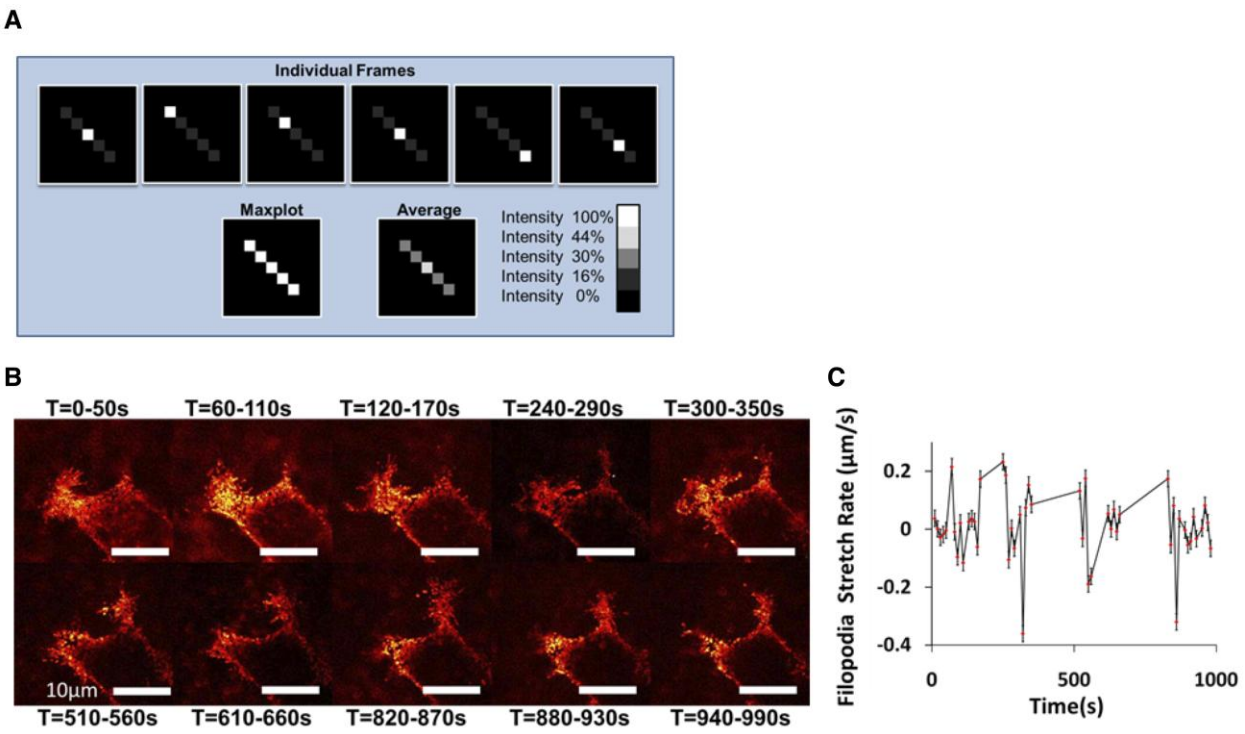

Figure S7, related to Figure 4. Maxplot Analysis of Na_Vs as labeled by STX-Cy5 in Filopodia in an NGF Differentiated PC12 Cell

(**A**) Maxplot analysis schematic. (**B**) Wide-field time-lapsed sequence of maxplot images using STX-Cy5. Each image is a maxplot average of data stacks acquired over 50 s. (**C**) Stretch rates of filopodia in (**A**) over 990 s showing a maximum stretch rate of 360 nm/s and an average rate of 80 ± 90 nm/s.

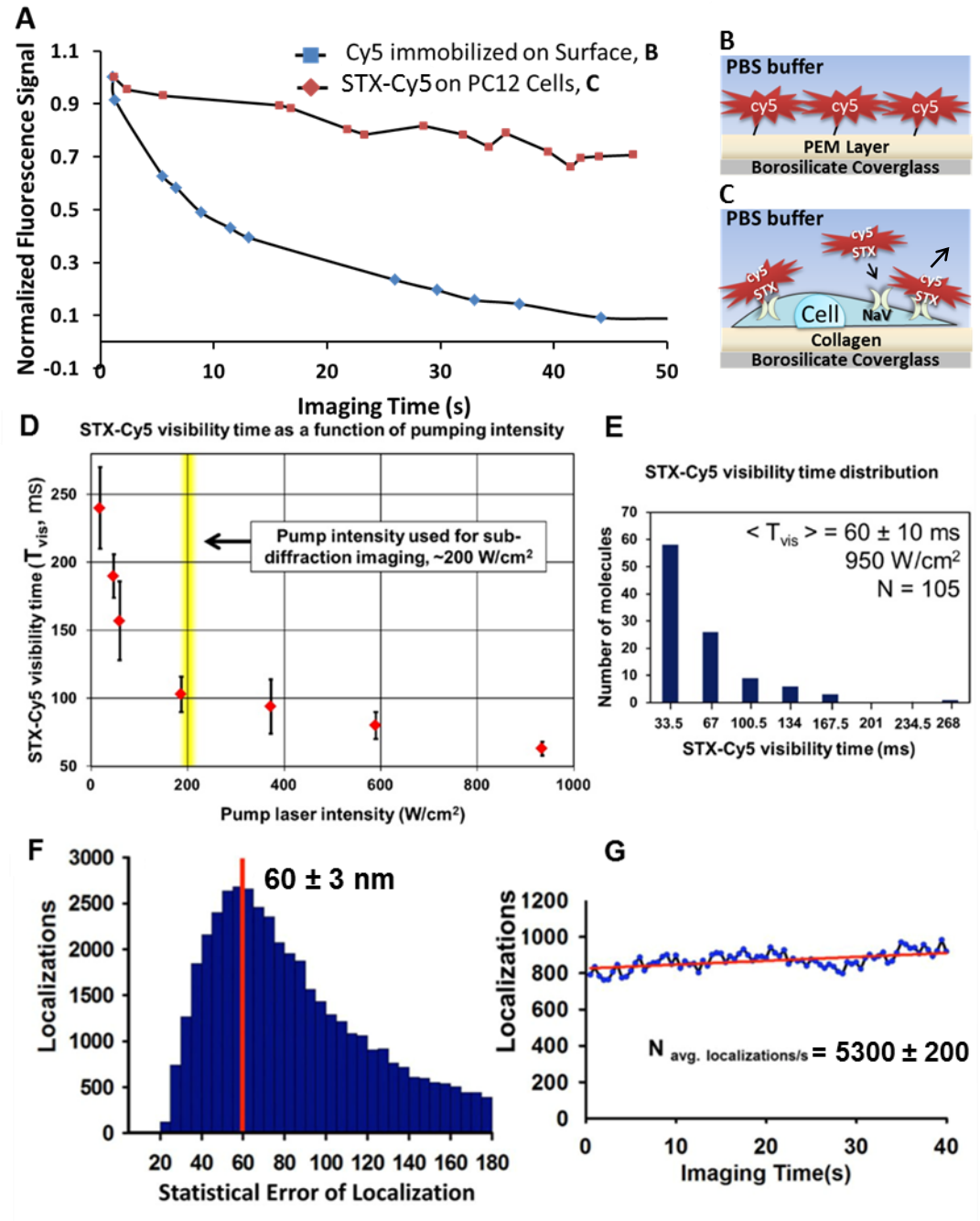

Figure S8, related to Figure 4 and Figure 5. Characterization of STX-Cy5 Fluorescence on Na_Vs in the Membrane of NGF Differentiated PC12 Cells

(**A**) Fluorescence intensities over time of **STX-Cy5** on Na_Vs in the membrane of NGF differentiated PC12 cells and of surface immobilized Cy5. Immobilized Cy5 signal decays exponentially over time while binding of new **STX-Cy5** from the medium to Na_Vs affords sustained fluorescence at the cell membrane. (**B**) Cy5 immobilized on a polyelectrolyte

multilayer. (**C**) New **STX-Cy5** from solution bind to Na_Vs in the cell membrane. (**D**)–(**E**) Variation of **STX-Cy5** visibility time (T_{vis}) at the membrane of NGF differentiated PC12 cells as a function of pump laser intensity. (**D**) **STX-Cy5** visibility time (T_{vis}) at the membrane at different pump laser intensities. (**E**) Visibility time distribution for single molecules at ~950 W/cm^2; the curve for 200 W/cm^2 is provided in the main text. The single-molecule **STX-Cy5** visibility time is significantly shorter at high pumping intensities, suggesting photobleaching as the primary cause for disappearance of the **STX-Cy5** signal. (**F**)–(**G**) Statistical localization precision and number of localizations over time of **STX-Cy5** bound to Na_Vs in the membrane of NGF differentiated PC12 cells. (**F**) The peak mode for the statistical error of localization at 96% confidence interval is 60 ± 3 nm. (**G**) New **STX-Cy5**–Na_V binding events afford an average of 5300 localizations per second.

Super-Resolution Weighted Moving Average Movie

Movie S1. Quasi-Real-Time Sub-Diffraction Reconstruction Movie of Na_Vs Labeled with 10 nM STX-Cy5 on a Neurite of an NGF Differentiated PC12 Cell

The movie shows the dynamic movements of neuritic spines. Single molecules of **STX-Cy5** from raw images acquired at 50 ms/frame were super-localized with a mean statistical localization precision of 25 ± 3 nm. The movie was generated from reconstructed sub-diffraction images using a weighted moving average algorithm and is displayed at 20 frames/second.

Supplementary Experimental Procedures

Synthesis of Fluorescent Saxitoxin Derivatives

Synthetic Procedures and Characterization Data

General: All reagents were obtained commercially unless otherwise noted. Reactions were performed using oven-dried glassware under an atmosphere of nitrogen. Air- and moisture sensitive liquids and solutions were transferred via syringe or stainless steel cannula. Organic solutions were concentrated under reduced pressure (ca. 15 Torr) by rotary evaporation. Aqueous solutions were concentrated under reduced pressure (ca. 0.05 Torr) at low temperature (ca. –60 °C) by lyophilization. Acetonitrile (MeCN) was passed through two columns of activated alumina immediately prior to use. **STX-NH_3^+** was prepared according to the procedure of Andresen (Andresen and Du Bois, 2009). **Cy5-NHS** was prepared according to the procedure of Kvach (Kvach et al., 2008). **DCDHF-NHS** was prepared according to the procedure of Wang (Wang, 2007). Stock solutions of **STX-Cy5** and **STX-DCDHF** in sterile filtered phosphate buffered saline (PBS, 500 nM) were aliquoted and stored at –20 °C in the dark. Semi-preparative high performance liquid chromatography (HPLC) was performed on a Varian ProStar model 320. Proton nuclear magnetic resonance (^{1}H NMR) spectra were acquired on a Varian Inova spectrometer operating at 500 MHz or on a Varian Inova spectrometer operating at 600 MHz and are referenced internally according to residual solvent signal. Data are recorded as follows: chemical shift (δ, ppm), multiplicity (s, singlet; d, doublet; t, triplet; q, quartet; quint, quintet; m, multiplet; br, broad), integration, coupling constant (Hz). High-resolution mass spectra were obtained from the Vincent Coates Foundation Mass Spectrometry Laboratory at Stanford University.

STX-Cy5: ^{1}H NMR (D_2O, 400 MHz) δ 8.01-7.94 (m, 2H), 7.50-7.47 (m, 2H), 7.41-7.37 (m, 2H), 7.24 (t, 4H, J = 7.6 Hz), 6.51 (t, 1H, J = 12.8 Hz), 6.23 (d, 1H, J = 2.4 Hz), 6.20 (d, 1H, J = 2.4 Hz), 4.64 (d, 1H, J = 1.2 Hz), 4.10 (dd, 1H, J = 11.6, 9.2 Hz), 4.97 (t, 2H, J = 6.4 Hz), 3.81 (dd, 1H, J = 11.6, 5.6 Hz), 3.75 (ddd, 1H, J = 10.0, 10.0, 2.4 Hz), 3.69 (dd, 1H, J = 9.2, 6.0 Hz), 3.54 (s, 3H), 3.48 (dd, 1H, J = 18.0, 10.0 Hz), 3.00-2.93 (m, 4H), 2.37 (ddd, 1H, J = 14.0, 8.4, 2.4 Hz), 2.29 (ddd, 1H, J = 13.6, 10.4, 10.4 Hz), 2.15 (t, 2H, J = 6.4 Hz), 1.85-1.78 (m, 2H), 1.62

(s, 6H), 1.62 (s, 6H), 1.61-1.54 (m, 2H), 1.37-1.24 (m, 6H), 1.20-1.16 (m, 2H) ppm (Figure 1B); HRMS (ES^+) calculated for $C_{48}H_{67}N_{10}O_5$ 863.5290 found 430.7580 ($MH^{2+}/2$).

STX-DCDHF: ^1H NMR (D_2O, 500 MHz) δ 7.73 (d, 1H, *J* = 16.5 Hz), 7.55 (d, 2H, *J* = 8.0 Hz), 6.82 (d, 2H, *J* = 8.5 Hz), 6.57 (d, 1H, *J* = 15.5 Hz), 4.68 (s, 1H), 4.20 (dd, 1H, *J* = 11.0, 11.0 Hz), 3.96 (dd, 1H, *J* = 10.5, 4.5 Hz), 3.78-3.73 (m, 2H), 3.53-3.48 (m, 3H), 3.08 (s, 3H), 3.01-2.99 (m, 4H), 2.38 (dd, 1H, *J* = 14.0, 5.6 Hz), 2.33-2.25 (m, 3H), 1.97-1.92 (m, 2H), 1.41-1.36 (m, 2H), 1.33-1.28 (m, 2H), 1.22-1.17 (m, 4H) ppm (Figure 1B); HRMS (ES^+) $C_{39}H_{50}N_{12}O_6$ 782.3976 found 392.4728 ($MH^{2+}/2$).

Fluorescence Enhancement of STX-DCDHF in Cell Suspension

PC12 cells were treated with 100 ng/mL NGF for 3 days, detached from culture flasks, pelleted, and re-suspended in PBS to provide a cell suspension of ~5 × 10^6 cells/mL. The fluorescence emission of **STX-DCDHF** (12.8 μM) in cell suspension was measured and compared to the fluorescence emission of **STX-DCDHF** (12.8 μM) in PBS (Figure S2B). The approximate 10× fluorescence enhancement in cell suspension is a unique emission property that stems from the viscosity and polarity sensitivity of the DCDHF chromophores and the likelihood that this molecule binds in cell membranes (Wang, 2007). For single-molecule experiments this property affords favorable signal-to-background ratios for **STX-DCDHF** relative to **STX-Cy5** on cell surfaces even at somewhat higher **STX-DCDHF** concentrations in solution.

Electrophysiology

On/Off Rates for Toxin Block

Approximate on times for Na_V block by **STX**, **STX-Cy5**, and **STX-DCDHF** were measured by applying solutions at saturating concentrations to NGF differentiated PC12 cells until complete Na^+ current block was observed. Off times for current recovery from block by each toxin were measured by perfusing with external solution until the original current was restored. Manual toxin application and wash off were performed at a constant rate of ~1 mL/min through a fast exchange diamond bath perfusion chamber (Warner instruments, Hamden, CT). Rate constants for Na^+ block (k_{on}) and recovery (k_{off}) for each toxin were derived from the Langmuir model for STX binding and calculated according to the equations (Hahn and Strichartz, 1981):

$$k_{on} = (1 / \tau_{on} - 1 / \tau_{off}) / [\text{toxin}]$$

$$k_{off} = 1 / \tau_{off}$$

where τ_{on} and τ_{off} are the measured times to complete block and current recovery, respectively, and [toxin] is the saturating concentration for each toxin (Figure S3).

Confocal and Wide-Field Epifluorescence Microscopy

For pre-block of STX-probe fluorescence by STX, evaluation of probe wash off, and analysis of PC12 ± NGF fluorescence, average laser power was measured using a FieldMaster GS power/energy analyzer (Coherent, Auburn, CA) and images were collected at constant laser transmission and acquisition settings. Fluorescence images were collected as a set of 10 z-stacks traversing the cells and projected as a composite. Quantification was performed using Volocity software; regions of interest corresponding to the perimeter of the cells were manually selected to obtain voxel counts. All intensities were corrected for background fluorescence. Data analysis and plotting were performed using Igor Pro software.

STX Pre-block of Fluorescence

PC12 cells were induced to differentiate with NGF for 4–7 days and placed in media containing 100 ng/mL NGF in the presence or absence of a pre-blocking concentration of 10 μM STX. Following 30 min incubation, aliquots of **STX-Cy5** or **STX-DCDHF** were added to each plate to yield final concentrations of 10 or 15 nM, respectively. Cells were incubated for an additional 15 min, then fluorescence images were acquired over a 15 min period. This procedure was repeated using 3 different sets of ± STX pre-block samples for each STX-fluorophore. Three areas on each plate containing 90–120 cells were imaged (examples for **STX-Cy5**: Figure 2A and 2B). Absolute fluorescence intensities were quantified as described above and normalized to the average fluorescence emission from cells in plates containing STX (Figure S4A).

Evaluation of Probe Wash Off

PC12 cells were induced to differentiate with NGF for 4–7 days and placed in media containing 100 ng/mL NGF and 10 nM **STX-Cy5** or 15 nM **STX-DCDHF**. Following 15 min incubation, pre-wash off images were acquired over a 15 min period. Media was removed, cells were washed with dye-free media (3×), and post-wash off images were acquired over a 15 min period. This procedure was repeated using 5 different plates for each STX-fluorophore. Three areas on each plate containing 90–120 cells were imaged both pre- and post-wash off (examples for **STX-Cy5**: Figure 2C and 2D). Absolute fluorescence intensities were quantified as described above and normalized to the average intensity of the corresponding pre-wash off images (Figure S4B). Sample areas were selected at random before and after wash off; each image represents a unique population of cells.

Fluorescence Measurements on PC12 ± NGF

PC12 cells were incubated in the presence or absence of NGF for 4–7 days and placed in media containing 10 nM **STX-Cy5** or 15 nM **STX-DCDHF**. For NGF differentiated cells, the media also contained 100 ng/mL NGF. Cells were incubated for 15 min and fluorescence images were acquired. This procedure was repeated using 5 different sets of ± NGF samples for each STX-fluorophore. Three areas on each plate containing 90–120 cells were imaged (examples for **STX-Cy5**: Figure 2E and 2F). Absolute fluorescence intensities were quantified as described above and normalized to the average fluorescence emission from NGF differentiated cells (Figure S4C).

Assessment of STX-Fluorophore Internalization

PC12 cells were induced to differentiate with NGF for 4–7 days and placed in media containing 100 ng/mL NGF and 10 nM **STX-Cy5** or 15 nM **STX-DCDHF**. Confocal z-stack images of 10–15 randomly selected cells on each plate were acquired at 63x after 15 min and 6 h (Figure S4D). No significant intracellular fluorescence emission was observed in any of the assayed cells at these time points.

Antibody Colocalization

PC12 cells were plated on borosilicate coverglass and induced to differentiate with NGF for 2 days, then washed with cold PBS buffer at pH 7.4 and fixed for 15 min using 3.7% paraformaldehyde in PBS at 4 °C. The paraformaldehyde solution was replaced by rinsing 4 times with fresh PBS. Fixed cells were permeabilized/pre-blocked with a solution containing 0.15% Triton-X 100 (Omnipur, EMD, Gibbstown, New Jersey), 1.5% BSA (Sigma-Aldrich, St. Louis, Missouri), and 10% fetal calf serum in PBS for 1 h at room temperature. Permeabilized cells were treated with 1 μg/mL primary antibody (rabbit polyclonal anti-pan rNa_V, Spring Bioscience, Pleasanton, CA) in pre-block solution for 8 h at room temperature. Cells were rinsed 4 times with fresh PBS and treated with pre-block solution for an additional 1 h. Following the second pre-block step, cells were treated with a secondary antibody conjugated to Alexa488 (Alexa Fluor488 goat anti-rabbit IgG (H+L), Invitrogen, San Diego, California) for 6 h at 4 °C. Cells were then washed 5 times with PBS and treated with 10 nM **STX-Cy5** or 15 nM **STX-DCDHF** in PBS for 15 min before imaging. Confocal images were acquired sequentially in multi-track mode and detected through a HFT UV/488/543/633 dichroic beam splitter with a 650 nm long-pass filter for **STX-Cy5** and **STX-DCDHF** and a HFT 488 dichroic beam splitter with a 500–550-nm IR bandpass filter for Alexa488 (Figure 2G–L).

Manders Overlay Coefficient Analysis

Three regions of interest (ROIs) were selected for images of NGF differentiated PC12 cells labeled with either 15 nM **STX-DCDHF** or 10 nM **STX-Cy5**. Fluorescence images at two emission wavelengths (**STX-Cy5**/**STX-DCDHF**, and Alexa488) were collected as a set of 10 z-stacks traversing the cells and every sub-stack was used in this quantification. Quantification was performed using an ImageJ plugin (JACoP v2.0). Averages of Manders colocalization coefficients over the 10 stacks of the 3 different ROIs are reported for each STX-fluorophore. In every sub-stack, the Manders coefficient (Bolte and Cordelieres, 2006) was calculated using the following equation:

$$M_{STX,Antibody} = \sum P_{STX,\,colocalized} / \sum P_{STX} \;,\; P_{STX,\,co\text{-}localized} = P_{STX} \;\; if \;, I_{antibody} \; of \; P_{STX} > 0$$

Briefly, Manders coefficient *M* is defined by summing intensities of colocalizing pixels from one channel and dividing by the integrated intensity from the other channel. A pixel *P* from the STX-fluorophore channel is considered to be colocalized if it has a non-zero intensity counterpart in

the antibody channel. As a result, Manders coefficient gives an estimate of the amount of colocalizing signal from the STX-fluorophore channel over the antibody channel without making any assumptions regarding stoichiometry. A value of 1.0 for Manders colocalization indicates perfect colocalization.

Confocal Imaging of CHO ± rNa$_V$1.4

Wild-type CHO cells were plated on plastic 6-well plates in 2 mL media and grown to 40–50% confluency. Cells were transfected with an expression vector containing the full-length cDNA coding for rat Na$_V$1.4 (rNa$_V$1.4) sodium channel α-subunit using the method of calcium phosphate precipitation; cotransfection with eGFP was used as a marker of transfection efficiency. Transfected cells were allowed to grow for 48 h, plated and grown on glass bottom dishes for 2 h until adherent, and incubated in media containing 40 nM **STX-Cy5** or 60 nM **STX-DCDHF** for 15 min prior to data collection. Samples of untransfected CHO cells were prepared in the same fashion. Confocal images were acquired sequentially in multi-track mode and detected through a HFT UV/488/543/633 dichroic beam splitter with a 650 nm long-pass filter for **STX-Cy5** and **STX-DCDHF** and a HFT 488 dichroic beam splitter with a 500–550 nm IR bandpass filter for eGFP.

The majority of cells expressing eGFP (cytosolic) also showed membrane labeling by the STX-fluorophores, and vice versa. Smaller populations of cells showing exclusively eGFP expression or STX-fluorophore binding were also visible (Figure S5A). Untransfected cells did not show specific membrane labeling.

rNa$_V$1.4 Plasmid Information

The nucleotide sequence of the rNa$_V$1.4 gene used in these studies (sequenced by Sequetech Corporation, Mountain View, CA) was aligned with the published gene sequences of the two channel isoforms, Na$_V$1.7 (GenBank accession no. AAB50403) and Na$_V$1.2 (GenBank accession no. NM_012647), induced in NGF differentiated PC12 cells using a FASTA sequence comparison program (University of Virginia; http://fasta.bioch.virginia.edu/fasta_www2/fasta_list2.shtml). This analysis shows nucleotide identities of 70.7% for rNa$_V$1.4 and Na$_V$1.7 (PC12) and 70.0% for rNa$_V$1.4 and Na$_V$1.2 (PC12),

and confirms that the proteins are nearly identical in the pore region surrounding the key residues responsible for STX binding (D400, E755, K1237, and A1529, $Na_V1.4$ numbering) (Figure S5C).

Time-Course of Ensemble Fluorescence Wash Off

PC12 cells were plated on borosilicate coverglass and induced to differentiate with NGF for 3 days. To establish background fluorescence, growth media was replaced with dye-free media and cells were imaged for 250 ms using the wide-field epi-illumination set-up described below (see **Single-Molecule Microscopy Instrumentation** under **Results** in the main text), with an excitation intensity of ~7 W/cm^2 at 633 nm. Cells were then incubated in media containing 2 μM of **STX-Cy5** for 10 minutes. After incubation, the **STX-Cy5** containing media was aspirated and a 250 ms frame of the PC12 membrane was recorded to establish single-frame bulk-level fluorescence intensity at t = 0. The sample was then perfused with external solution for electrophysiology (see **Electrophysiology Acquisition Protocols** under **Results** in the main text) at 1 mL/min using a cassette pump. During the course of perfusion, fluorescence images were periodically acquired to monitor the fluorescence signal at the cell membrane (Figure S6). The sample was protected from laser illumination between acquisition time points to minimize the effects of photobleaching. For each trial, the individual fluorescence intensity measurement was normalized by first subtracting cellular autofluorescence then dividing by fluorescence intensity at t = 0. Figure S6 presents the average time-course of ensemble fluorescence wash off from 3 separate trials. The time necessary to wash away **STX-Cy5** from the differentiated PC12 is on the same order of magnitude as the **STX-Cy5** off rates measured by electrophysiology (see **Electrophysiology On/Off Rates for Toxin Block** under **Results** in the main text).

Single-Molecule and Super-Resolution Microscopy

Single-Molecule Wide-Field Imaging of CHO ± $rNa_V1.4$

Wild-type CHO cells were transfected with $rNa_V1.4$ and eGFP using the lipofectamine method and incubated for 24 h prior to epifluorescence imaging. In addition to the 633 and 594 nm laser lines used to excite **STX-Cy5** and **STX-DCDHF**, a 488 nm Argon ion laser was used in the excitation path to aid in finding CHO cells expressing eGFP. Operationally, CHO cells exhibiting eGFP fluorescence were deemed likely to have been successfully transfected with the

rNa$_V$1.4 plasmid. In representative populations of sampled cells, STX-fluorophore signals were observed only in CHO cells expressing eGFP. No STX-fluorophore signal was observed on the surfaces of CHO cells that were not transfected (Figure S5B).

Maxplot Analysis of Na$_V$s and Stretch Measurements in Filopodia

From raw image stacks, maxplot images were obtained using ImageJ function Z Project with maximum intensity. Briefly, this function takes the highest intensity a pixel exhibits through time as the intensity of that pixel (Figure S7A).

Filopodium length was defined as the distance between the terminus of soma and the tip of filopodium shown by an arrow in the upper right of the image (Figure S7B). For frames summed over 10 s, the soma and filopodium termini positions were measured by hand. The positions were measured in triplicate and error bars defined as 2× the standard deviation of these measurements. Filopodia stretch rates were determined by dividing the absolute value of the change in filopodium length by the elapsed time (10 s). This stretch measurement included both extension and retraction. The maximum stretch rate observed over the length of 990 s was 360 nm/s with an average stretch rate of 80 ± 90 nm/s, consistent with reported filopodia extension rates in neurons (Figure S7C; see Mallavarapu and Mitchison, 1999; Lu et al., 1997; Sheetz et al., 1992; Kress et al., 2007; Costantino et al., 2008; Laishram et al., 2009 under **References** in the main text).

Single Particle Tracking

NGF differentiated PC12 cells were labeled with 12.8 nM **STX-DCDHF**. All movies were recorded at 50 ms integration time with continuous epifluorescence illumination. The successive (x,y) positions of single molecules in the plane of the cell surface were recorded as a function of time. To investigate the behavior of single Na$_V$s in a consistent fashion, only the fluorescent spots that appeared after the start of illumination and disappeared before the end of recording were considered. The residence time (τ_R) was defined as the time from the initial appearance of a single-molecule spot on the membrane (from the solution) to the time of its disappearance from the imaging focal plane in a single frame.

Trajectories of single STX-fluorophores were extracted by using a Single Particle Tracking (SPT) program from ETH-Zurich (now available as the ImageJ plugin http://www.mosaic.ethz.ch/Downloads/ParticleTracker; a previous Java version was used for these studies) (Sbalzarini and Koumoutsakos, 2005). In this analysis, particle positions were iteratively refined using the intensity centroid for sub-pixel interpolation. Trajectories were computationally extracted from the recorded movie sequences using a feature-point tracking algorithm described previously (Lee et al., 2008; Qian et al., 1991). All trajectories were visually inspected to ensure that the tracking program was operating properly. The mean-squared displacement from each individual single-molecule trajectory (truncated to 10 time steps, typically at 0.050 s per time step) was used to extract an observed short-time diffusion coefficient *D*. Each single-molecule trajectory produced an apparent diffusion coefficient, *D*, which was regarded as an estimate of the true diffusion coefficient of the particles. The distribution of apparent diffusion coefficients for the individual trajectories was generated to test for heterogeneity in the motion. To perform this test, an estimate of error was needed. Under the hypothesis that all molecules are moving as unconstrained Brownian diffusers, the distribution of measurements of *D* is as follows (Biteen et al., 2008):

$$p(D)dD = \frac{1}{(N-1)!}\cdot\left(\frac{N}{D_o}\right)^N\cdot(D)^{N-1}\cdot\exp\left(\frac{-ND}{D_o}\right)\cdot dD$$

where *D* is the diffusion coefficient extracted from an individual trajectory, D_0 is the underlying Brownian diffusion coefficient, and *N* is the number of time steps in each trajectory. This expression was used to generate the smooth curves in the text by fixing $N = 10$ and using the arithmetic mean of the observed *D* values for D_0.

Evaluation of STX-Cy5 for Target-Specific PAINT

Cy5 molecules were immobilized on a polyelectrolyte multilayer *via* ligation of **Cy5-NHS** to exposed lysine residues on the multilayer surface. The fluorescence emission of immobilized Cy5 in dye-free PBS was measured over 50 s and compared to the corresponding emission of **STX-Cy5** at the cell membrane of an NGF differentiated PC12 cell in a solution containing ~10 nM **STX-Cy5**. Whereas new binding events of **STX-Cy5** molecules from solution to Na_Vs at the

PC12 cell membrane afforded sustained fluorescence signal over time, immobilized Cy5 exhibited a characteristic exponential decay in fluorescence signal (Figure S8A).

The visibility time (T_{vis}) of **STX-Cy5** at the membrane of NGF differentiated PC12 cells was measured at different laser pump intensities from 20 W/cm^2 to 950 W/cm^2. The observed decay in visibility time with increasing laser intensity with an approximate hyperbolic shape implies that photobleaching and possibly intensity-dependent blinking are significant pathways contributing to signal disappearance (Figure S8D). Here, the efficient "turn off" events necessary to maintain a sparse, resolvable subset of emitters required for pointillist super-resolution imaging schemes are provided by binding of **STX-Cy5** to Na_Vs followed by rapid photobleaching of the bound probe.

These data show that binding of new STX-fluorophores results in the replenishing of single-molecule signals and contributes efficient turn on events (see **Super-Resolution Localization and Reconstruction** below). The constant replenishing of fluorescent probes to cell surface Na_Vs (Figure S8B and 8C) combined with efficient photobleaching (Figure S8A) is responsible for the observed turn on/off. That is, the binding of **STX-Cy5** followed by rapid photobleaching of the bound **STX-Cy5** and binding of new **STX-Cy5** from solution affords the efficient turn on/off behavior required for pointillist super-resolution imaging schemes. This imaging approach can be regarded as a target-specific version of PAINT (Points Accumulation for Imaging in Nanoscale Topography), as described in the main text.

Super-Resolution Localization and Reconstruction

From raw image stacks, super-resolution images were obtained using previously published image processing techniques as described (Biteen et al., 2008). Briefly, for each imaging frame, the position of the single emitter was determined by fitting the signal above background in a small region of interest containing the single-molecule spot to a two-dimensional Gaussian with non-linear least squares regression analysis (**nlinfit**, in MATLAB). Each single-molecule point spread function (PSF) was fit to determine the following parameters: **background**, **amplitude**, **width**, **center(x) and center(y)**. Fits with a localization precision greater than 212 nm were also discarded. The resulting statistical error of localization at 96% confidence interval (2× standard

deviation) was found to have a peak mode at 60 ± 3 nm (Figure S8F). To reconstruct a super-resolution image, each single-molecule position was re-plotted using a custom macro written in ImageJ as a two-dimensional Gaussian having a constant amplitude and σ (standard deviation or width) equal to the average standard deviation error of the center of the fit, i.e. 30 nm (from 60 nm ÷ 2). This is a conservative value to use as compared to the theoretical mean statistical localization precision of our data. The theoretical mean statistical localization precision is described by the following equation (Thompson et al., 2002):

$$\sigma = \sqrt{\frac{s^2 + a^2/12}{N} + \frac{8\pi s^4 b^2}{a^2 N^2}}$$

where s is the standard deviation of the Gaussian fit to the PSF, a is the pixel size, N is the number of photons, and b is the background noise. In these data we obtained an s of 340 nm, an N of 4640 ± 1800 photons/frame, a pixel size of 107 nm, and b of 21 ± 1 photons/pixel. Using these parameters, the theoretical mean statistical localization precision was ~25 ± 3 nm, smaller than the width used in our reconstructions (30 nm). Since every molecule was plotted identically, the brightness in the plot is reasonably proportional to the density of STX binding events. Lastly, given the 50 ms exposure time, and 5300 localizations/s as afforded by the new binding events of **STX-Cy5** (Figure S8G), 5 s was sufficient to reconstruct a representation of a neurite projection.

At a focal depth of ~500 nm and >10 nM concentration of STX-fluorophore in solution, we would expect signal-to-background ratio of approximately < 10:1 in a single diffraction-limited spot assuming perfect filtering and background arising only from diffusing fluorophores in solution. Given additional background from cellular autofluorescence and the usual losses in emission filters, the signal-to-background in our experiments (1.8 ± 0.4 for **STX-Cy5**, and 4.2 ± 0.5 for **STX-DCDHF**) is reasonable.

Super-Resolution Movie

A weighted moving average procedure was used to generate a sliding quasi-real-time movie. Super-resolution reconstructions in 50 ms time frames were first generated using a custom ImageJ macro written to plot the localizations in each frame as xy-scatter plots, followed by filtering by a two-dimensional Gaussian filter with kernel size 1.2 pixels. The following time-weighting algorithm was then used to generate averaged frames, each with ten 50 ms frames combined and plotted as 1 frame.

$$F'_{(k)} = \sum_{n=0}^{9} \left[F_{(k-n)} \times \left(1 - \frac{n}{10} \right) \right]$$

In this formalism, *F'(k)* is the new frame with frame number k, and *F(n)* is the original reconstructed super-resolution 50 ms frame. As a result of this weighting algorithm, the brightest colored two-dimensional Gaussian spots are from the most recent frame within the weighting window ensemble (Movie S1).

Supplemental References

Andresen, B.M., and Du Bois, J. (2009). De novo synthesis of modified saxitoxins for sodium ion channel study. J. Am. Chem. Soc. *35*, 12524–12525.

Biteen, J.S., Thompson, M.A., Tselentis, N.K., Bowman, G.R., Shapiro, L., and Moerner, W.E. (2008). Superresolution imaging in live Caulobacter crescentus cells using photoswitchable EYFP. Nat. Methods *5*, 947–949.

Bolte, S., and Cordelieres, F.P. (2006). A guided tour into subcellular colocalization analysis in light microscopy. J. Microscopy *224*, 213–232.

Hahn, R., and Strichartz G (1981). Effects of deuterium oxide on the rate and dissociation constants for saxitoxin and tetrodotoxin action. J. Gen. Physiol. *78*, 113–139.

Kvach, M. V., Ustinov, A. V., Stepanova, I. A., Malakhov, A. D., Skorobogatyi, M. V., Shmanai, V. V., and Korshun, V. A. (2008). A convenient synthesis of cyanine dyes: reagents for the labeling of biomolecules. Eur. J. Org. Chem. *2008*, 2107–2117.

Lee, H.L., Dubikovskaya, E.A., Hwang, H., Semyonov, A.N., Wang, H., Jones, L.R., Twieg, R.J., Moerner, W.E., and Wender, P.A. (2008). Single-molecule motions of oligoarginine conjugates on the plasma membrane of Chinese Hamster Ovary cells. J. Am. Chem. Soc. *130*, 9364–9370.

Qian, H., Sheetz, M.P., and Elson, E.L. (1991). Single particle tracking. Analysis of diffusion and flow in two-dimensional systems. Biophys. J. *60*, 910–921.

Sbalzarini, I.F., and Koumoutsakos, P. (2005). Feature point tracking and trajectory analysis for video imaging in cell biology. J. Struct. Biol. *151*,182–195.

Thompson, R.E., Larson, D.R., and Webb, W.W. (2002). Precise nanometer localization analysis for individual fluorescent probes. Biophys. J. *82*, 2775–2783.

Wang. H (2007). Tuning DCDHF (dicyanomethylenedihydrofuran) fluorophores and their applications in biological systems. PhD Thesis, Kent State University.